

A REFINED HIGHER-ORDER GENERALLY ORTHOTROPIC C^0 PLATE BENDING ELEMENT

B. N. PANDYA and TARUN KANT

Department of Civil Engineering, Indian Institute of Technology, Powai, Bombay 400 076, India

(Received 28 August 1986)

Abstract—A finite element formulation for flexure of a generally orthotropic plate based on a higher-order displacement model and a three-dimensional state of stress and strain is presented here. This higher-order theory incorporates linear variation of transverse normal strain/stress and parabolic variation of transverse shear strains through the thickness of the plate. The nine-noded quadrilateral from the family of two-dimensional C^0 continuous isoparametric Lagrangian elements is then developed as a generally orthotropic higher-order element. The performance of this element is evaluated on square plates with different support conditions and under uniformly distributed and central point loads. The numerical results of the present formulation are compared with thin plate, elasticity and Mindlin/Reissner solutions. The effect of degree of orthotropy on the maximum bending moment location is examined for different loading and boundary conditions. The effect of directional orthotropy on the location of the maximum values for the various stress-resultants is also studied.

INTRODUCTION

It is an established fact that the classical thin plate theory [1, 2] based on the so-called Kirchhoff hypothesis is computationally inefficient from the point of view of simple finite element formulations [3, 4]. Besides, it is based on simplifying assumptions, the most important of which are the neglect of the transverse shear deformations and the transverse normal stress. The errors in such a theory naturally increase as the plate thickness increases. In addition, due to neglect of transverse shear deformations and transverse normal stress, one cannot take into account all of the nine stiffness coefficients in the constitutive relation of a general orthotropic material. Consequently, the errors increase as the magnitude of inplane stiffness increases relative to the transverse stiffness of the material in general. For instance, in plates with a a/h ratio less than 10 and a high degree of orthotropy involving a large ratio of E_x/E_y , Ashton and Whitney [5] have reported enormous discrepancy in the results of the classical thin plate theory.

Reissner [6] and Mindlin [7] were the first to provide first-order shear deformable theories based on the thin plate assumptions for variation of stresses and displacements through the thickness of the plate, respectively. Both these theories give rise to a sixth-order partial differential system of equilibrium equations and permit satisfaction of three boundary conditions on each edge. Medwadowski [8] extended Reissner's theory (based on assumed stress fields) to orthotropic plates. Yang *et al.* [9], on the other hand, extended Mindlin's theory (based on assumed displacement fields) to heterogeneous plates.

The foregoing theories provide a first-order basis for the consideration of the effects of the transverse shear deformations on the behaviour of isotropic,

orthotropic and heterogeneous plates and these also yield a C^0 continuous finite element formulation for the numerical analysis but have certain limitations: the transverse shearing strains (and thereby stresses) are assumed constant through the plate thickness and a fictitious shear correction coefficient is introduced; the classical contradiction whereby both the transverse normal stress (σ_z) and the transverse normal strain (ϵ_z) are neglected, remains unresolved. Lo *et al.* [10, 11] and Reissner [12] presented a theory for plates based on an assumed higher-order displacement field. Kant [13] derived an isotropic version of the complete governing equations of such a theory in a systematic manner based on the minimum potential energy principle and has also compared it with Mindlin theory through extensive numerical studies. Kant *et al.* [14] also presented, for the first time, a C^0 finite element formulation of this higher-order theory. Specifically, the in-plane and the transverse displacements are expanded in the powers of the thickness coordinate (z) by Taylor series and the truncations are effected at the third and the second degrees respectively. The theory thus incorporates: (i) quadratic variation of the transverse shearing strains (γ_{xz} and γ_{yz}) through the plate thickness, making the introduction of a shear correction coefficient redundant; (ii) linear variation of the transverse normal strain (ϵ_z) through the plate thickness; and (iii) consideration of the three-dimensional Hooke's law. Motivation for the present study comes from these works in the form of an extension for generally orthotropic plates.

Recently Phan and Reddy [15] presented a finite element formulation of a plate theory based on an assumed displacement field of Levinson [16] and Murthy [17] in which in-plane displacements are expanded as cubic functions of the thickness co-

ordinate while the transverse deflection is kept only a function of x and y (independent of thickness coordinate) as assumed in the case of classical and Mindlin/Reissner plate theory. The additional four higher-order functions used in the definition of the in-plane displacements are eliminated and expressed in terms of the usual physical lower-order displacement functions of the classical/Reissner/Mindlin theory by conditioning that the transverse shear stresses are zero on the bounding planes of the plate. Implicit in this development is the use of only a partial constitutive relation which ignores the contributions and effects of transverse normal stress (σ_z)/strain (ϵ_z). The resulting formulation is also seen to contain second-order derivatives, as in the classical plate theory, of the transverse deflection (w) in the energy expression and consequently the displacement based finite element formulation requires the use of computationally inefficient C^1 continuous shape functions.

Further, with present increasing interest in the use of composite materials in high technology areas, it is important that we predict reliably their failure/fracture mode. Failure phenomenon in composite materials is extremely complex. Nevertheless, delamination mode of the failure is now recognised as the

except the terms θ_x^* , θ_y^* and w^* , which are the corresponding higher-order terms in the Taylor's series expansion, used in the present theory and are defined at the reference plane. Thus the generalized displacement vector δ of the reference plane is defined as

$$\delta = \{w, \theta_x, \theta_y, w^*, \theta_x^*, \theta_y^*\}^t \quad (2)$$

The strains, in terms of displacement vector δ are expressed as

$$\begin{aligned} \epsilon_x &= z\kappa_x + z^3\kappa_x^* \\ \epsilon_y &= z\kappa_y + z^3\kappa_y^* \\ \epsilon_z &= z\kappa_z \\ \gamma_{xy} &= z\kappa_{xy} + z^3\kappa_{xy}^* \\ \gamma_{xz} &= \phi_y + z^2\phi_y^* \\ \gamma_{yz} &= \phi_x + z^2\phi_x^* \end{aligned} \quad (3)$$

The generalized strain components vector $\bar{\epsilon}$ is related to the generalized displacement components δ by the following matrix relation:

$$\bar{\epsilon} = \begin{Bmatrix} \kappa_x \\ \kappa_y \\ \kappa_{xy} \\ \kappa_x^* \\ \kappa_y^* \\ \kappa_{xy}^* \\ \kappa_z \\ \phi_x \\ \phi_y \\ \phi_x^* \\ \phi_y^* \end{Bmatrix} = \begin{bmatrix} 0 & \partial/\partial x & 0 & 0 & 0 & 0 & 0 & 0 & 0 & 0 & 0 \\ 0 & 0 & \partial/\partial y & 0 & 0 & 0 & 0 & 0 & 0 & 0 & 0 \\ 0 & \partial/\partial y & \partial/\partial x & 0 & 0 & 0 & 0 & 0 & 0 & 0 & 0 \\ 0 & 0 & 0 & 0 & \partial/\partial x & 0 & 0 & 0 & 0 & 0 & 0 \\ 0 & 0 & 0 & 0 & 0 & \partial/\partial y & 0 & 0 & 0 & 0 & 0 \\ 0 & 0 & 0 & 0 & 0 & \partial/\partial y & \partial/\partial x & 0 & 0 & 0 & 0 \\ 0 & 0 & 0 & 2 & 0 & 0 & 0 & 0 & 0 & 0 & 0 \\ \partial/\partial x & 1 & 0 & 0 & 0 & 0 & 0 & 0 & 0 & 0 & 0 \\ \partial/\partial y & 0 & 1 & 0 & 0 & 0 & 0 & 0 & 0 & 0 & 0 \\ 0 & 0 & 0 & \partial/\partial x & 3 & 0 & 0 & 0 & 0 & 0 & 0 \\ 0 & 0 & 0 & \partial/\partial x & 0 & 3 & 0 & 0 & 0 & 0 & 0 \end{bmatrix} \begin{Bmatrix} w \\ \theta_x \\ \theta_y \\ w^* \\ \theta_x^* \\ \theta_y^* \end{Bmatrix} = \mathbf{L}\delta \quad (4)$$

most critical one [18]. Initiation and/or growth of this failure mode is due to inter-laminar stresses τ_{xz} , τ_{yz} , and also σ_z , which is not considered by Phan and Reddy [15], Levinson [16] and Murthy [17].

We believe that the present formulation, though cumbersome [17], has the potential to predict all six components of the stress tensor accurately and is thus worth pursuing.

HIGHER-ORDER ELEMENT FORMULATION

The theory is based on the displacement model,

$$\begin{aligned} U(x, y, z) &= z\theta_x(x, y) + z^3\theta_x^*(x, y) \\ V(x, y, z) &= z\theta_y(x, y) + z^3\theta_y^*(x, y) \\ W(x, y, z) &= w(x, y) + z^2w^*(x, y), \end{aligned} \quad (1)$$

in which the various terms have the usual meaning

The total potential energy π for the present theory [14] is given by

$$\pi = \frac{1}{2} \int_A \bar{\epsilon}^T \bar{\sigma} dA - \int_A (p_z^+ + p_z^-) \left(w + \frac{h^2}{4} w^* \right) dA, \quad (5)$$

where p_z^+ and p_z^- are the transverse distributed loads on the positive and negative extreme z planes respectively and h is the total thickness of the plate. The generalized stress component vector $\bar{\sigma}$, which is the integral of the physical stress components through the thickness of the plate, is given by

$$\bar{\sigma} = \{M_x, M_y, M_{xy}, M_x^*, M_y^*, M_{xy}^*, M_z, Q_x, Q_y, Q_x^*, Q_y^*\}^t \quad (6)$$

The generalized stress vector $\bar{\sigma}$ and the generalized strain vector $\bar{\epsilon}$ are partitioned as follows:

$$\bar{\sigma} = \{\bar{\sigma}_b, \bar{\sigma}_s\}^t \quad \text{and} \quad \bar{\epsilon} = \{\bar{\epsilon}_b, \bar{\epsilon}_s\}^t \quad (7)$$

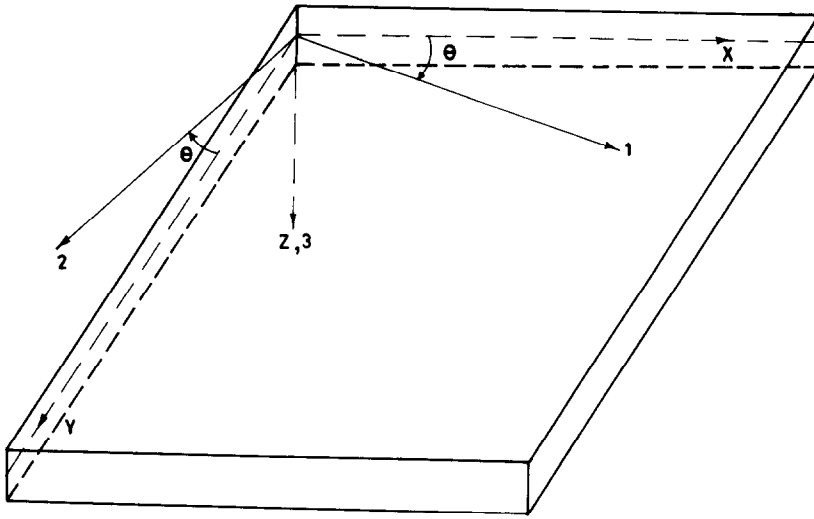


Fig. 1. Positive system of coordinates.

where

$$\bar{\sigma}_b = \{M_x, M_y, M_{xy}, M_x^*, M_y^*, M_{xy}^*, M_z\}'$$

$$\bar{\sigma}_s = \{Q_x, Q_y, Q_x^*, Q_y^*\}' \tag{8}$$

$$\bar{\epsilon}_b = \{\kappa_x, \kappa_y, \kappa_{xy}, \kappa_x^*, \kappa_y^*, \kappa_{xy}^*, \kappa_z\}'$$

$$\bar{\epsilon}_s = \{\phi_x, \phi_y, \phi_x^*, \phi_y^*\}' \tag{9}$$

For a linear elastic material the constitutive relation can be written as

$$\bar{\sigma}_b = \mathbf{D}_b \bar{\epsilon}_b \text{ and } \bar{\sigma}_s = \mathbf{D}_s \bar{\epsilon}_s, \tag{10}$$

where the elasticity matrices \mathbf{D}_b and \mathbf{D}_s for a general orthotropic plate of thickness h are expressed in the following manner:

$$\epsilon = \begin{Bmatrix} \epsilon_1 \\ \epsilon_2 \\ \epsilon_3 \\ \gamma_{12} \\ \gamma_{23} \\ \gamma_{13} \end{Bmatrix} = \begin{bmatrix} 1/E_1 & -\nu_{12}/E_1 & -\nu_{13}/E_1 & 0 & 0 & 0 \\ -\nu_{21}/E_2 & 1/E_2 & -\nu_{23}/E_2 & 0 & 0 & 0 \\ -\nu_{31}/E_3 & -\nu_{32}/E_3 & 1/E_3 & 0 & 0 & 0 \\ 0 & 0 & 0 & 1/G_{12} & 0 & 0 \\ 0 & 0 & 0 & 0 & 1/G_{23} & 0 \\ 0 & 0 & 0 & 0 & 0 & 1/G_{13} \end{bmatrix} \begin{Bmatrix} \sigma_1 \\ \sigma_2 \\ \sigma_3 \\ \tau_{12} \\ \tau_{23} \\ \tau_{13} \end{Bmatrix} = \mathbf{S}\sigma. \tag{13}$$

$\mathbf{D}_b =$

$$\begin{bmatrix} Q_{11}H_1 & Q_{12}H_1 & Q_{14}H_1 & Q_{11}H_2 & Q_{12}H_2 & Q_{14}H_2 & Q_{13}H_1 \\ & Q_{22}H_1 & Q_{24}H_1 & Q_{12}H_2 & Q_{22}H_2 & Q_{24}H_2 & Q_{23}H_1 \\ & & Q_{44}H_1 & Q_{14}H_2 & Q_{24}H_2 & Q_{44}H_2 & Q_{34}H_1 \\ & & & Q_{11}H_3 & Q_{12}H_3 & Q_{14}H_3 & Q_{13}H_2 \\ & & & & Q_{22}H_3 & Q_{24}H_3 & Q_{23}H_2 \\ \text{Symm.} & & & & & Q_{44}H_3 & Q_{34}H_2 \\ & & & & & & Q_{33}H_1 \end{bmatrix} \tag{11}$$

$$\mathbf{D}_s = \begin{bmatrix} Q_{66}h & Q_{56}h & Q_{66}H_1 & Q_{56}H_1 \\ & Q_{55}h & Q_{56}H_1 & Q_{55}H_1 \\ & & Q_{66}H_2 & Q_{56}H_2 \\ \text{Symm.} & & & Q_{55}H_2 \end{bmatrix}, \tag{12}$$

in which

$$H_1 = h^3/12$$

$$H_2 = h^5/80$$

$$H_3 = h^7/448.$$

The coefficients Q_{ij} ($i, j = 1-6$) in terms of nine independent elastic constants are derived as follows.

The three-dimensional strains ϵ are related to stresses σ by a compliance matrix \mathbf{S} with respect to the 1-2-3 set of co-ordinate axes (see Fig. 1):

By inverting the compliance matrix, the stiffness matrix \mathbf{C} , relating stresses and strains, is obtained as

$$\sigma = \mathbf{S}^{-1}\epsilon = \mathbf{C}\epsilon. \tag{14}$$

The coefficients of \mathbf{C} matrix are given in Appendix 1. Next, the stress vector, strain vector and stiffness matrix are transformed from the 1-2-3 set of axes to the x - y - z set of axes using the relation:

$$\bar{\sigma} = \mathbf{T}^{-1}\mathbf{C}[\mathbf{T}^{-1}]'\bar{\epsilon} = \mathbf{Q}\bar{\epsilon}, \tag{15}$$

where

$$\mathbf{T} = \begin{bmatrix} c^2 & s^2 & 0 & -2sc & 0 & 0 \\ s^2 & c^2 & 0 & 2sc & 0 & 0 \\ 0 & 0 & 1 & 0 & 0 & 0 \\ sc & -sc & 0 & c^2 - s^2 & 0 & 0 \\ 0 & 0 & 0 & 0 & c & -s \\ 0 & 0 & 0 & 0 & s & c \end{bmatrix} \quad (16)$$

(in which $c = \cos \theta$ and $s = \sin \theta$) is the transformation matrix, $\bar{\sigma}$ and $\bar{\epsilon}$ are the stresses and strain vectors respectively, with respect to the x - y - z axes. The coefficients of \mathbf{Q} matrix are given in Appendix 2.

The generalized displacement vector δ and nodal displacement vector δ_i are related with the aid of shape function N_i as follows:

$$\delta = \sum_{i=1}^n N_i \delta_i, \quad (17)$$

where n = total number of nodes/element. With the generalized displacement vector, δ , known at all points within the element, the generalized strain vector $\bar{\epsilon}$ at any point is derived with the help of eqns (4) and (17) as follows:

$$\bar{\epsilon} = \mathbf{L}\delta = \mathbf{L} \sum_{i=1}^n N_i \delta_i = \sum_{i=1}^n \mathbf{B}_i \delta_i, \quad (18)$$

where

$$\mathbf{B}_i = \mathbf{L}N_i. \quad (19)$$

The elasticity matrix \mathbf{D} is expressed as

$$\mathbf{D} = \begin{bmatrix} \mathbf{D}_b & | & 0 \\ \hline 0 & | & \mathbf{D}_s \end{bmatrix}, \quad (20)$$

where \mathbf{D}_b and \mathbf{D}_s matrices are already expressed in eqns (11) and (12) respectively. Having obtained the \mathbf{D} and \mathbf{B} matrices as given by eqns (19) and (20), respectively, the element stiffness matrix \mathbf{K}^e can be readily computed by using the standard relation

$$\mathbf{K}_{ij}^e = \int_{A^e} \mathbf{B}_i^T \mathbf{D} \mathbf{B}_j dA = \int_{-1}^{+1} \int_{-1}^{+1} \mathbf{B}_i^T \mathbf{D} \mathbf{B}_j |\mathbf{J}| d\xi d\eta. \quad (21)$$

The computation of the element stiffness matrix is economised by explicit multiplication of the \mathbf{B}_i , \mathbf{D} and \mathbf{B}_j matrices instead of carrying out the full matrix multiplication of the triple product, and due to symmetry of the stiffness matrix only the blocks \mathbf{K}_{ij} lying on one side of the main diagonal are formed [14, 19].

The formulation for consistent load vector \mathbf{P} remains the same as given in [14].

NUMERICAL EXAMPLES

For numerical computations of various types of examples, a computer program has been developed

which incorporates present higher-order theory. Simultaneously, a computer program based on Mindlin's theory [20] has been executed to support the numerical evaluations of the present theory.

For all the numerical examples, a quarter plate is discretized with four of the nine-noded Lagrangian quadrilateral elements. The selective integration scheme based on Gauss-Legendre product rules, viz. 3×3 and 2×2 , has been employed for flexural and shear contributions respectively to compute the element stiffness matrix. The numerical study consists of the following examples.

Example 1

In this example, a square orthotropic plate ($\theta = 0$) of side $a = 1$ and subjected to a transverse uniform load $p = 1$ is analysed with simply supported ($w = \theta, w^* = \theta^* = 0$) boundary conditions. Srinivas and Rao [21] have solved this problem assuming the following elastic rigidities:

$$\frac{Q_{22}}{Q_{11}} = 0.543103$$

$$\frac{Q_{33}}{Q_{11}} = 0.530172$$

$$\frac{Q_{12}}{Q_{11}} = 0.233190$$

$$\frac{Q_{13}}{Q_{11}} = 0.010776$$

$$\frac{Q_{23}}{Q_{11}} = 0.098276$$

$$\frac{G_{12}}{Q_{11}} = 0.262931$$

$$\frac{G_{13}}{Q_{11}} = 0.159914$$

$$\frac{G_{23}}{Q_{11}} = 0.266810$$

and the same are used here; they have also presented solutions by Reissner's and thin plate theories.

Tables 1-3 compare the deflections, bending moments and transverse shear respectively, at the critical locations given by Srinivas and Rao with those obtained using present higher-order and Mindlin finite element formulations. The agreement for deflections and moments between the elasticity solution given by Srinivas and Rao and the present higher-order plate solution is much better compared to the Mindlin solution. For the above comparative study, the stress values given by Srinivas and Rao have been integrated through the thickness of the plate to calculate moment and shear stress resultants, assuming linear variation of direct stresses and parabolic variation for shear stress through the thickness

Table 1. Deflections in simply supported orthotropic plate ($\theta = 0^\circ$) under uniform loading

	$[w_{\max} E_x h^3 / pa^4]$ at center for different a/h					
	5.00	7.14	10.00	20.00	50.00	100.00
Present higher-order element	0.0830536	0.0735276	0.0689695	0.0653741	0.0643626	0.0642285
Mindlin element	0.0774328	0.0703612	0.0670297	0.0644127	0.0635896	0.0633045
Elasticity solution [21]	—	0.0734014	0.0688570	0.0652687	—	—
Reissner's theory [21]	—	0.0733822	0.0688370	0.0652625	—	—
Thin plate theory [21]	—	0.0640394	0.0640390	0.0640375	—	—
% Deviation w.r.t. thin plate value	—	-12.90	-7.15	-2.04	—	—
% Deviation w.r.t. Mindlin value	-6.77	-4.31	-2.81	-1.47	-1.20	-1.44

Table 2. Moments in simply supported orthotropic plate ($\theta = 0^\circ$) under uniform loading

	$(M_x \text{ or } M_y)$ at center/ pa^2 for different a/h					
	5.00	7.14	10.00	20.00	50.00	100.00
Present higher-order element	M_x	0.05734	0.05899	0.05981	0.06067	0.06064
	M_y	0.03903	0.03765	0.03698	0.03644	0.03629
	M_x	0.06095	0.06064	0.06046	0.06028	0.05995
Mindlin element	M_x	0.03653	0.03676	0.03687	0.03694	0.03681
	M_y	—	0.05993	0.06004	0.06013	—
	M_x	—	0.03794	0.03702	0.03628	—
Reissner's theory [21]	M_x	—	0.05849	0.05930	0.05995	—
	M_y	—	0.03603	0.03604	0.03604	—
	M_x	—	0.06016	0.06016	0.06016	—
Thin plate theory [21]	M_x	—	0.03603	0.03604	0.03604	—
	M_y	—	1.98	0.59	-0.51	—
	M_x	—	-4.30	-2.54	-1.10	—
% Deviation w.r.t. thin plate value	—	6.30	2.80	1.09	-1.14	-2.29
% Deviation w.r.t. Mindlin value	-6.41	-2.36	-0.30	1.37	1.43	0.41

Table 3. Transverse shear in simply supported orthotropic plate ($\theta = 0^\circ$) under uniform loading

	Q_x at mid-edge/ pa for different a/h					
	5.00	7.14	10.00	20.00	50.00	100.00
Present higher-order element	0.3131	0.3168	0.3184	0.3196	0.3194	0.3193
Mindlin element	0.3201	0.3194	0.3191	0.3190	0.3220	0.3288
Elasticity solution [21]	—	0.3483	0.3561	0.3624	—	—
Reissner's theory [21]	—	0.3616	0.3618	0.3621	—	—
Thin plate theory [21]	—	0.3720	0.3709	0.3657	—	—
% Deviation w.r.t. thin plate value	—	17.42	16.49	14.42	—	—
% Deviation w.r.t. Mindlin value	2.24	0.82	0.22	-0.19	0.81	2.98

of the plate. The agreement for transverse shear between two finite element solutions is better as compared with approximate calculations from shear stresses presented by Srinivas and Rao. In Tables 1-3, some additional results with $a/h = 5, 50$ and 100 are also presented.

Example 2

A square orthotropic plate ($\theta = 0$) of side $a = 1$ is analysed for two different loading conditions, viz.: (i) transverse uniform pressure $p = 1$; and (ii) central point load $P = 1$ with three different boundary conditions, namely, (a) simply supported (S), i.e. $w = \theta_x = w^* = \theta_x^* = 0$, (b) just supported (S*), i.e. $w = w^* = 0$, and (c) clamped (C), i.e. $w = \theta_x = \theta_n = w^* = \theta_n^* = \theta_n^* = 0$ for various degrees of orthotropy (E_x/E_y). The material properties considered for this example are listed in Figs 2-7.

Iyengar and Pandya [22] have presented an elasticity solution for simply supported plate under uniform pressure with different degree of orthotropy and a/h ratios. They have also presented results of

Ambartsumyan's and Reissner's theory. Table 4 compares the deflections at the center of the plate obtained by Iyengar and Pandya with those obtained using higher-order and Mindlin finite element formulations. It can be seen that for $E_x/E_y = 3$ and $a/h = 10$, agreement between present higher-order element and elasticity solutions is better as compared with Mindlin finite element formulation. For $E_x/E_y = 3$ with $a/h = 10, 5, 2.5$, both the finite element solutions agree with the elasticity solution. But, for $E_x/E_y = 40$ with $a/h = 10, 5, 2.5$, agreement between Mindlin element and elasticity solution is better compared to higher order elements. Tables 5 and 6 compare moments and transverse shear respectively at the critical locations. Tables 7 and 8 present two finite element results for deflections and moments respectively, for a plate under uniform pressure with $a/h = 100, E_x/E_y = 1$ (isotropic), 4, 5, 6, 10, 20, 40 and the three different boundary conditions stated above. Similar results for deflections and moments are presented in Tables 9 and 10 respectively, for a plate with central point load. From Table 8, it

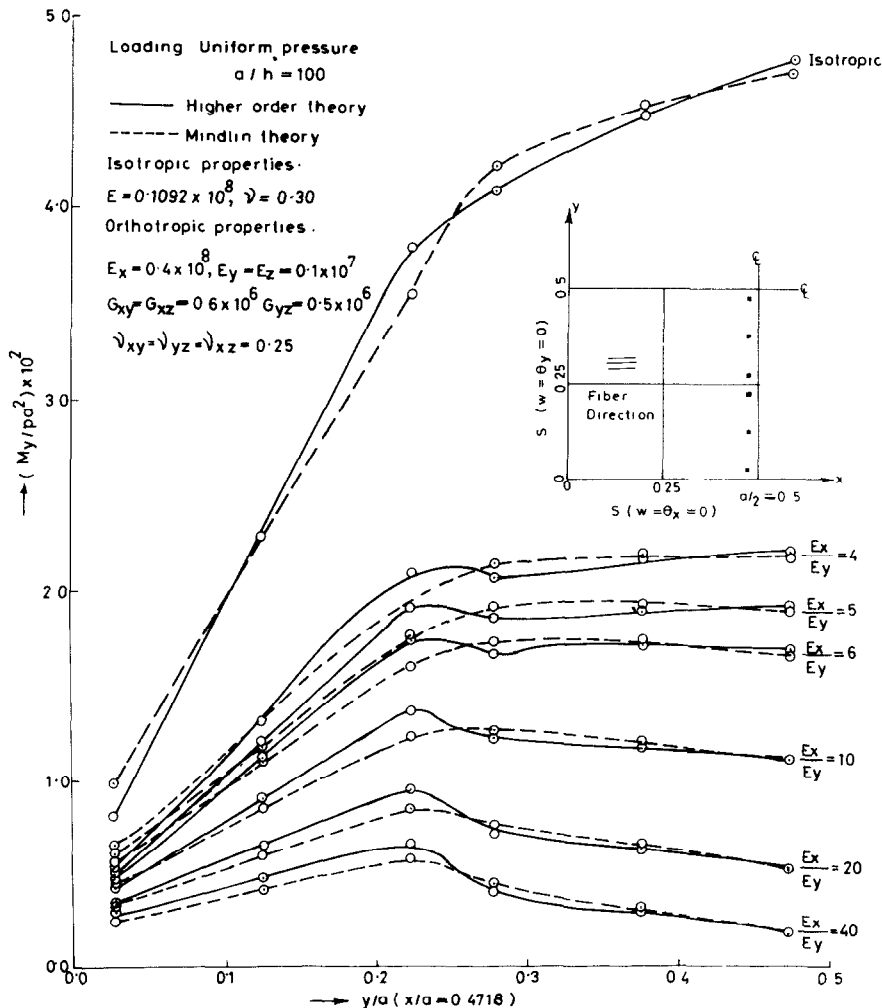


Fig. 2 Moment (M_y) variation in a simply supported plate under a uniformly distributed load.

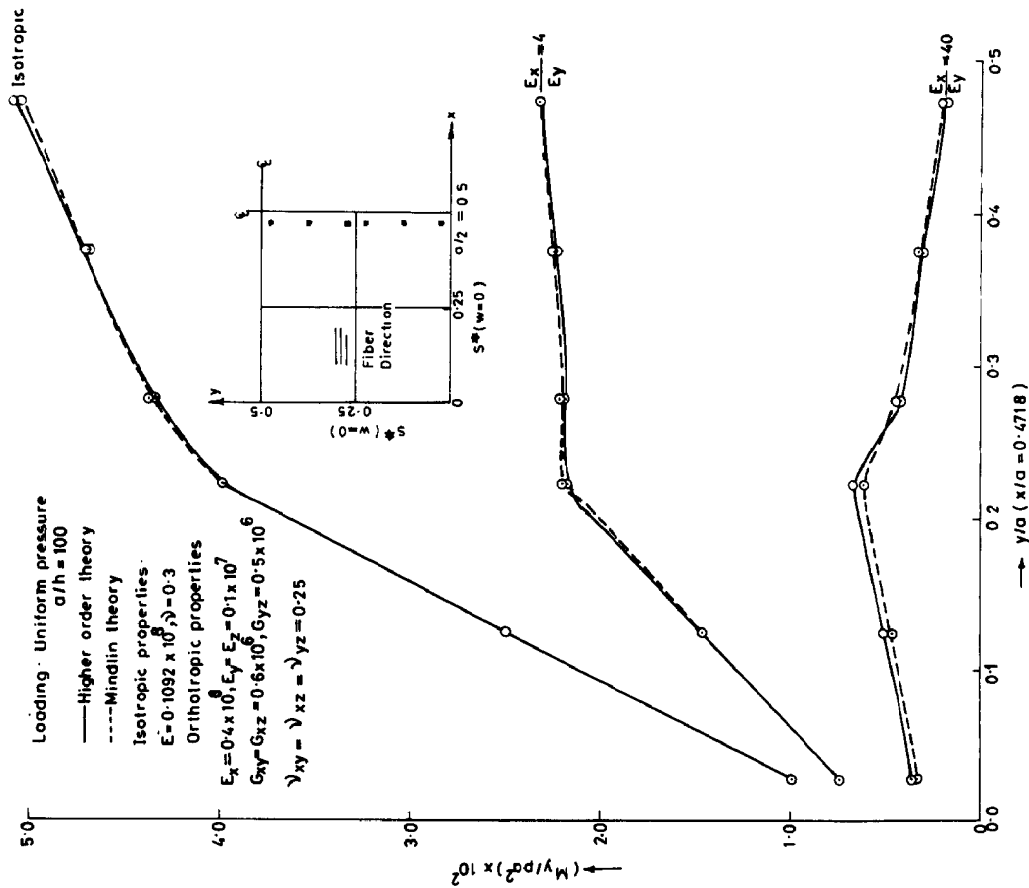


Fig. 3. Moment (M_y) variation in a just supported plate under a uniformly distributed load.

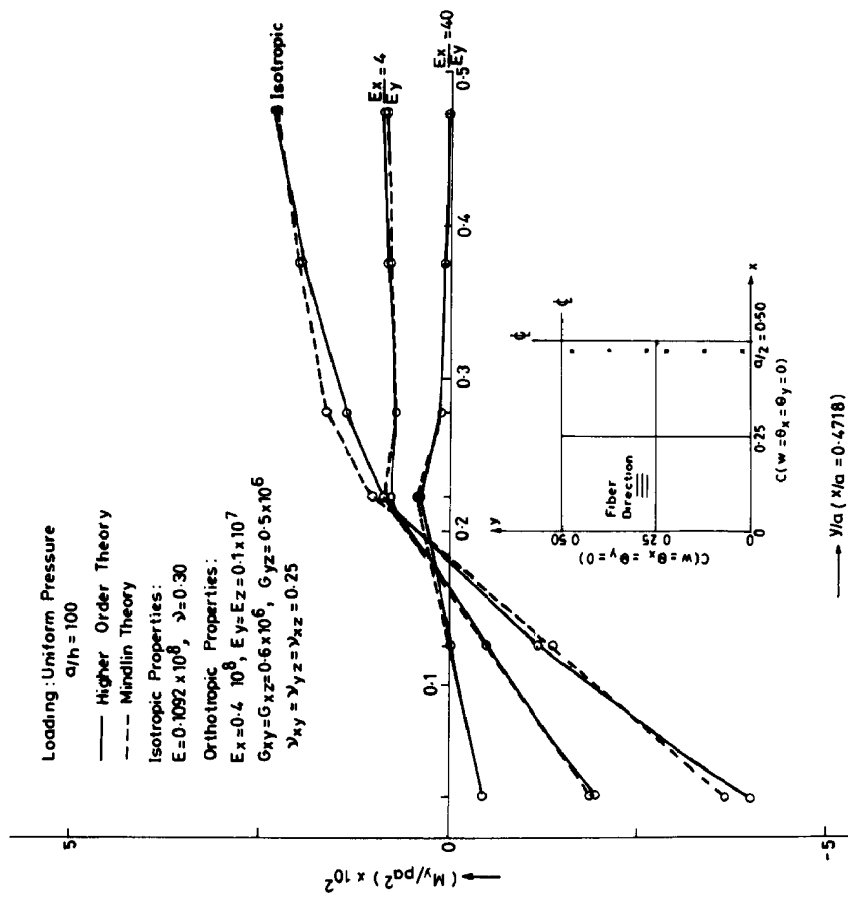


Fig. 4. Moment (M_y) variation in a clamped plate under a uniformly distributed load.

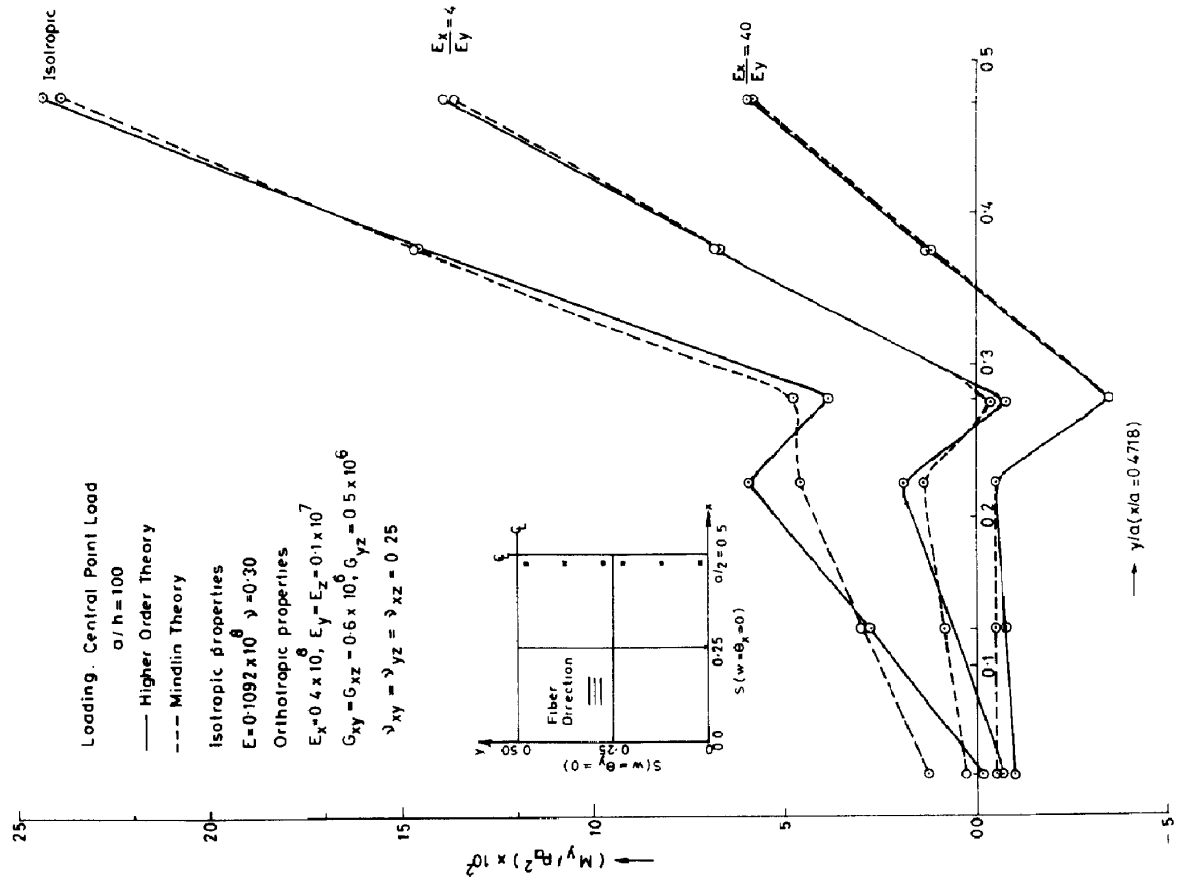


Fig. 5 Moment (M_y) variation in a simply supported plate under a central point load

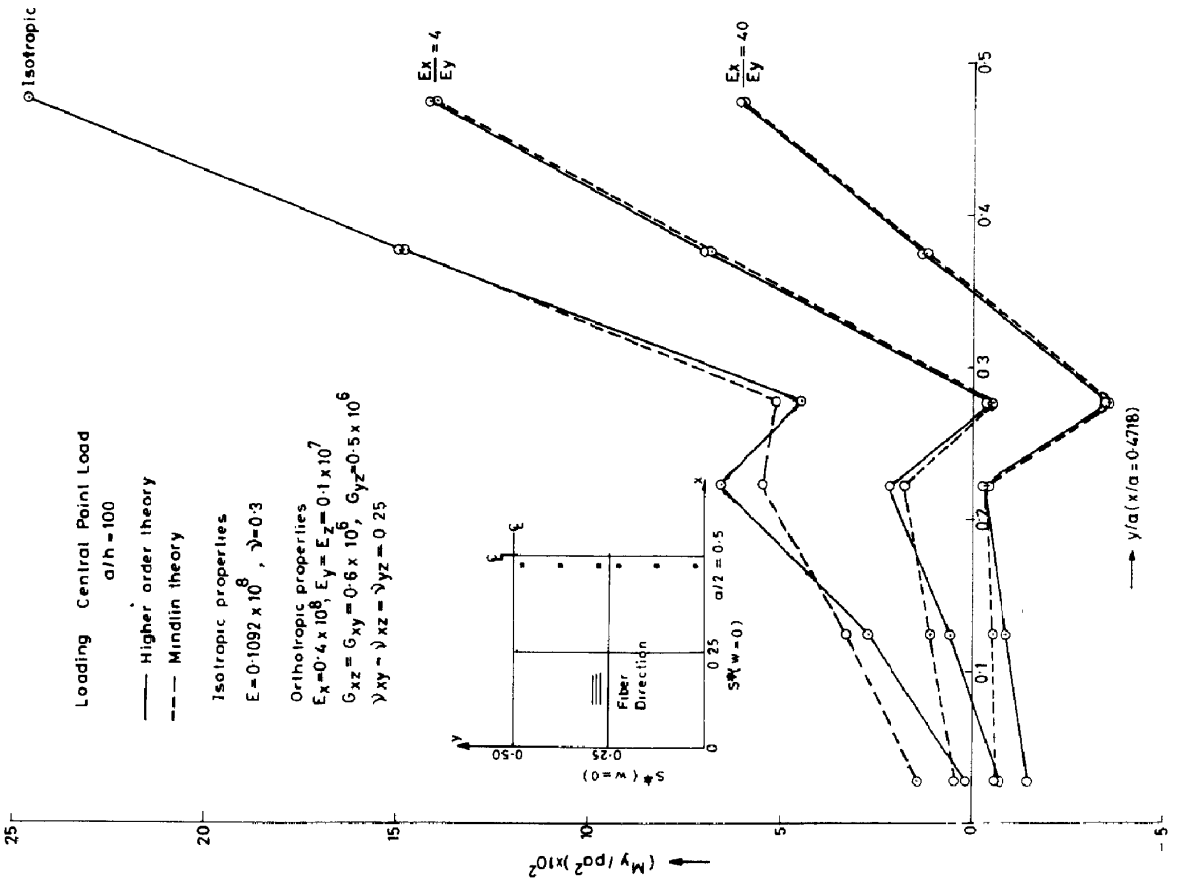


Fig. 6 Moment (M_y) variation in a just supported plate under a central point load

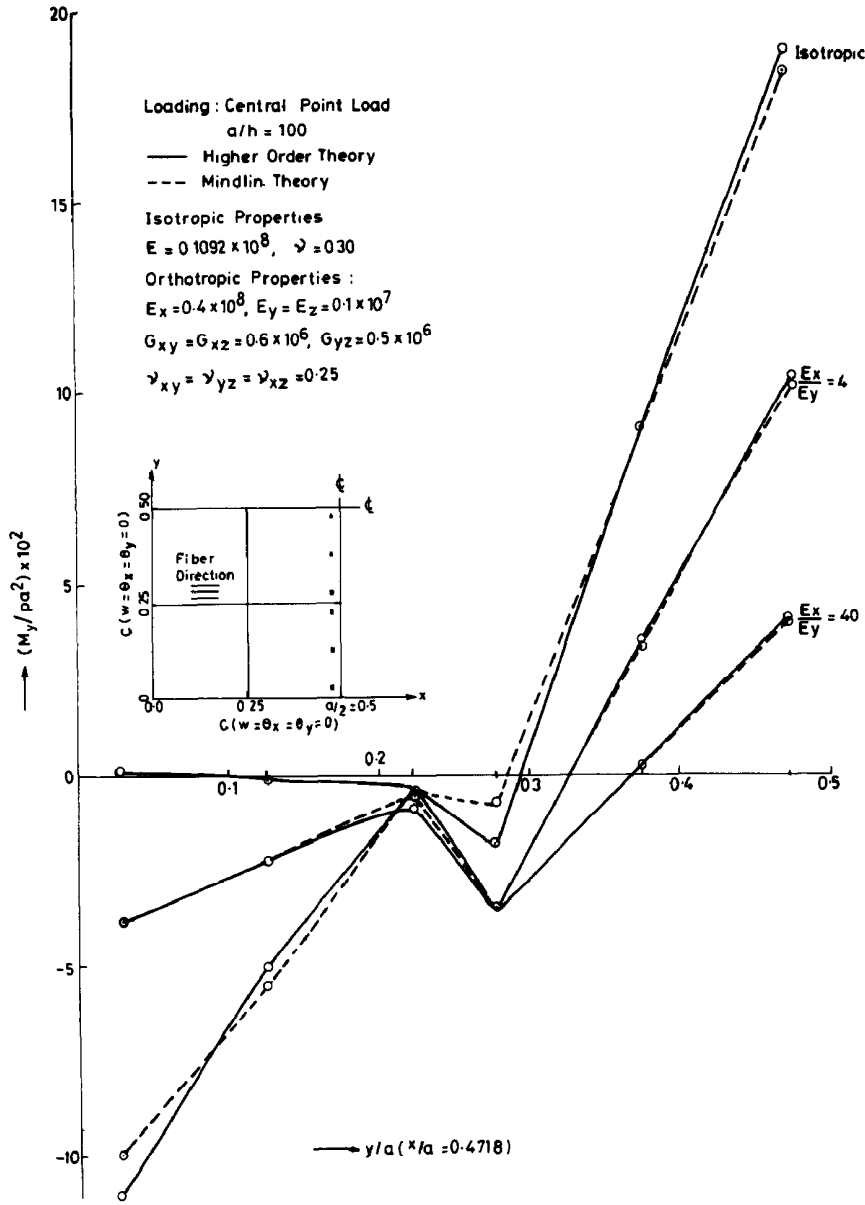


Fig. 7. Moment (M_y) variation in a clamped plate under a central point load.

Table 4. Deflections in simply supported orthotropic ($\theta = 0^\circ$) plate under uniform loading

$\frac{E_x}{E_y}$	$\frac{a}{h}$	$\left[\frac{E_y \cdot w_{max}}{ph} \right]$ at center				
		Present higher-order element	Mindlin element	Method of initial functions [22]	Ambartsumyan's theory [22]	Reissner's theory [22]
3	10.0	294.12	293.27	293.78	294.81	293.31
	5.0	21.27	21.20	21.36	21.56	21.18
	2.5	2.02	2.02	2.12	2.12	2.03
10	10.0	158.14	158.19	158.22	158.52	157.82
	5.0	13.59	13.68	13.85	13.77	13.58
	2.5	1.65	1.69	1.86	1.75	1.69
40	10.0	67.34	67.70	67.82	67.69	67.49
	5.0	8.68	8.90	9.20	8.90	8.81
	2.5	1.41	1.52	1.81	1.55	1.51

Table 5. Moments in simply supported orthotropic plate ($\theta = 0^\circ$) under uniform loading

E_x/E_y	a/h	Max(M_x, M_y or M_{xy})/ pa^2			Mindlin element		
		Present higher-order element			Mindlin element		
		M_x	M_y	$-M_{xy}$	M_x	M_y	$-M_{xy}$
3	10.0	0.07192	0.02647	0.03135	0.07157	0.02645	0.03137
	5.0	0.07063	0.02785	0.03076	0.06950	0.02778	0.03195
	2.5	0.06725	0.03233	0.02807	0.06280	0.03193	0.03345
10	10.0	0.1114	0.01470*	0.01705	0.1114	0.01465*	0.01707
	5.0	0.1054	0.01704*	0.01819	0.1051	0.01705*	0.01912
	2.5	0.09016	0.02589	0.01957	0.08698	0.02523	0.02435
40	10.0	0.1341	0.008442*	0.007388	0.1344	0.008347*	0.00739
	5.0	0.1261	0.01232*	0.01013	0.1266	0.01222*	0.01095
	2.5	0.1036	0.02182	0.01455	0.1001	0.02164	0.01937

Max. BM values without * occur at center of the plate (nearest G.P) and those with * occur at (0.4718a, 0.2218a).

Max. TM occurs at corner of the plate (nearest G.P).

Table 6. Transverse shear in simply supported orthotropic plate ($\theta = 0^\circ$) under uniform loading

E_x/E_y	a/h	Max(Q_x or Q_y) at mid-edge/ pa			
		Present higher-order element		Mindlin element	
		Q_x	Q_y	Q_x	Q_y
3	10.0	0.3524	0.2189	0.3522	0.2196
	5.0	0.3489	0.2221	0.3481	0.2238
	2.5	0.3376	0.2331	0.3329	0.2387
10	10.0	0.4317	0.1377	0.4321	0.1380
	5.0	0.4188	0.1518	0.4200	0.1523
	2.5	0.3824	0.1890	0.3802	0.1925
40	10.0	0.4748	0.07993	0.4759	0.07964
	5.0	0.4594	0.1064	0.4622	0.1058
	2.5	0.4085	0.1620	0.4052	0.1673

Table 7. Deflections in orthotropic plate ($\theta = 0^\circ$) under uniform loading ($a/h = 100$)

Theory	BC	$\frac{E_x}{E_y}$	$\frac{w_{max} D}{pa^4} \times 10^2$						
			1 (Isotropic)	4	5	6	10	20	40
			$(w_{max} E_y h^3 / pa^4) \times 10^2$						
Higher-order	S		0.407	2.436	2.162	1.942	1.375	0.785	0.414
	S*		0.418	2.492	2.205	1.977	1.391	0.790	0.414
	C		0.123	0.654	0.558	0.485	0.316	0.165	0.082
Mindlin	S		0.404	2.422	2.151	1.933	1.372	0.787	0.418
	S*		0.418	2.494	2.207	1.979	1.394	0.794	0.418
	C		0.124	0.640	0.546	0.475	0.310	0.163	0.082

Table 8. Moments in orthotropic plate ($\theta = 0^\circ$) under uniform loading ($a/h = 100$)

Theory	BC	$\frac{E_x}{E_y}$	$(\text{Max } M_x \text{ or } M_y/pa^2) \times 10$						
			1 (Isotropic)	4	5	6	10	20	40
Higher-order	S ($w = \theta_t = 0$)	M_x	0.482	0.829	0.910	0.975	1.134	1.283	1.344
			(4,9)	(4,9)	(4,9)	(4,9)	(4,9)	(4,9)	(4,9)
		M_y	0.482	0.222	0.193	0.177	0.138	0.096	0.066
			(4,9)	(4,9)	(4,9)	(2,9)	(2,9)	(2,9)	(2,9)
	S*($w = 0$)	M_x	0.511	0.877	0.960	1.026	1.188	1.337	1.399
			(4,9)	(4,9)	(4,9)	(4,9)	(4,9)	(4,9)	(4,9)
		M_y	0.511	0.233	0.202	0.185	0.143	0.098	0.067
			(4,9)	(4,9)	(4,9)	(2,9)	(2,9)	(2,9)	(2,9)
	C ($w = \theta_t = \theta_n = 0$)	M_x	0.227	0.368	0.391	0.407	0.440	0.456	0.455
			(4,9)	(4,9)	(4,9)	(4,9)	(4,9)	(4,9)	(4,8)
		M_y	0.227	0.085	0.073	0.069	0.061	0.050	0.039
			(4,9)	(4,9)	(2,9)	(2,9)	(2,9)	(2,9)	(2,9)
$-M_x$		0.399	0.598	0.627	0.648	0.689	0.708	0.701	
		(3,3)	(3,3)	(3,3)	(3,3)	(3,3)	(3,3)	(3,2)	
$-M_y$	0.399	0.194	0.170	0.153	0.111	0.071	0.045		
Mindlin	S ($w = \theta_t = 0$)	M_x	0.473	0.818	0.901	0.966	1.131	1.290	1.363
			(4,9)	(4,9)	(4,9)	(4,9)	(4,9)	(4,9)	(4,9)
		M_y	0.473	0.221	0.195	0.175	0.134	0.090	0.059
			(4,9)	(4,8)	(4,8)	(2,6)	(2,6)	(2,6)	(2,6)
	S*($w = 0$)	M_x	0.506	0.874	0.958	1.026	1.194	1.354	1.428
			(4,9)	(4,9)	(4,9)	(4,9)	(4,9)	(4,9)	(4,9)
		M_y	0.506	0.232	0.201	0.181	0.138	0.092	0.061
			(4,9)	(4,9)	(4,9)	(2,9)	(2,9)	(2,9)	(2,9)
	C ($w = \theta_t = \theta_n = 0$)	M_x	0.219	0.344	0.366	0.382	0.418	0.443	0.452
			(4,9)	(4,9)	(4,9)	(4,9)	(4,9)	(4,8)	(4,8)
		M_y	0.219	0.081	0.082	0.079	0.069	0.055	0.041
			(4,9)	(4,9)	(2,9)	(2,9)	(2,9)	(2,9)	(2,9)
$-M_x$	0.366	0.575	0.603	0.624	0.666	0.690	0.700		
	(3,3)	(3,3)	(3,3)	(3,3)	(3,3)	(3,3)	(3,2)		
$-M_y$	0.366	0.189	0.166	0.150	0.110	0.070	0.044		
		(2,7)	(2,7)	(2,7)	(2,7)	(2,7)	(2,7)		

Note: Positions are specified by element No. and G.P. No. respectively within the bracket.

Table 9. Deflections in orthotropic plate ($\theta = 0^\circ$) with a central point load ($a/h = 100$)

Theory	BC	$\frac{E_x}{E_y}$	$\frac{w_{\text{max}} D}{pa^2} \times 10^2$						
			1 (Isotropic)	4	5	6	10	20	40
Higher-order	S		1.160	7.087	6.351	5.765	4.260	2.683	1.650
	S*		1.187	7.228	6.465	5.859	4.312	2.707	1.664
	C		0.550	3.093	2.706	2.414	1.724	1.071	0.663
Mindlin	S		1.143	6.981	6.257	5.677	4.190	2.631	1.612
	S*		1.173	7.131	6.372	5.770	4.235	2.645	1.618
	C		0.541	2.993	2.620	2.339	1.677	1.050	0.654

Table 10. Moments in orthotropic plate ($\theta = 0^\circ$) with a central point load ($a/h = 100$)

Theory	BC	$\frac{E_x}{E_y}$	(Max M_x or Max M_y/p) $\times 10$							
			1 (Isotropic)	4	5	6	10	20	40	
Higher-order	S	M_x	2.441	3.694	4.009	4.269	4.998	5.975	6.977	
		M_y	2.441	1.404	1.301	1.219	1.009	0.778	0.602	
	S*	M_x	2.483	3.739	4.048	4.302	5.004	5.926	6.856	
		M_y	2.483	1.427	1.320	1.237	1.002	0.789	0.612	
	C	M_x	1.886	2.272	2.901	3.049	3.464	4.037	4.634	
		M_y	1.886	1.036	0.948	0.882	0.717	0.539	0.399	
		$-M_x$	1.106	1.982	2.140	2.268	2.623	3.129	3.709 (4.7)	
		$-M_y$	1.106	0.376	0.378	0.389	0.404	0.391	0.351	
	Mindlin	S	M_x	2.384	3.582	3.890	4.145	4.866	5.829	6.811
			M_y	2.384	1.370	1.270	1.191	0.986	0.761	0.592
S*		M_x	2.467	3.692	3.999	4.252	4.956	5.875	6.797	
		M_y	2.467	1.411	1.305	1.222	1.010	0.778	0.605	
C		M_x	1.831	2.575	2.749	2.894	3.313	3.922	4.569	
		M_y	1.831	1.012	0.932	0.870	0.716	0.546	0.406	
		$-M_x$	0.996	1.852	2.000	2.121	2.464	2.983	3.608	
		$-M_y$	0.996	0.370	0.380	0.397	0.421	0.408	0.359	

Note: Unless otherwise specified by Ele. No. and G.P. No. respectively within the bracket, all max. positive BMs occur at centre of plate (nearest G.P.) and max. negative BMs occur at mid-edge (nearest G.P.).

can be seen that for a plate under uniform pressure positive moment in the fibre direction (M_x) is maximum at the center of the plate for all three boundary conditions considered except for clamped plate with $E_x/E_y = 40$. But, positive maximum moment in cross-fibre direction (M_y) shifts its location beyond a certain degree of orthotropy for different boundary conditions. From Table 10, it can be seen that this kind of differential trend is absent for a plate carrying central point load. For this loading case, locations for positive maximum moments in both the directions and for all the three boundary conditions remain at the center of the plate. The peculiar nature of the cross-fibre direction moment curves along the plate centre line (nearest Gauss point) in the same direction with different degree of orthotropy have been presented graphically in Figs 2-7.

Example 3

A square orthotropic plate ($\theta \neq 0$) of side $a = 1$ with $a/h = 10$ is analysed for uniform pressure load $p = 1$ and simply supported boundary conditions ($w = \theta_x = w^* = \theta_x^* = 0$) for various values of fibre orientation (θ). Hussainy and Srinivas [23] have solved this problem assuming the following elastic rigidities:

The elastic rigidities considered in this example are the same as above and the additional properties required in the present theory due to consideration of σ_z are calculated by assuming $E_2 = E_3$ and $\nu_{12} = \nu_{23} = \nu_{13}$. They have also presented thin plate results.

Table 11 compares the deflections and critical moments obtained by Hussainy and Srinivas with those obtained using higher-order and Mindlin elements. The agreement for both deflections as well as moments between the elasticity solution and the present higher-order element is better compared to Mindlin elements.

This example also includes a study of shifts for maximum stress resultant locations with the variations in fibre orientation. This is presented schematically in Figs 8-10 for (w, Q_x, Q_y, M_{xy}), M_x and M_y respectively. The material properties considered here are:

$$E_1 = 0.4215 \times 10^8,$$

$$E_2 = E_3 = 0.2169 \times 10^7,$$

$$G_{12} = G_{13} = 0.1001 \times 10^7,$$

$$G_{23} = 0.6 \times 10^6,$$

$$\nu_{12} = \nu_{23} = \nu_{13} = 0.2413.$$

Property	Orientation		
	30°	45°	60°
Q_{11}	24870370.0	12389410.0	4832576.0
Q_{22}	4832576.0	12389410.0	24870362.0
Q_{12}	7910705.0	10372566.0	7910701.7
G_{12}	8394336.0	10856304.0	8394334.3
G_{23}	696246.0	800305.0	904365.3
G_{13}	904363.0	800305.0	696246.1

CONCLUSIONS

A refined higher-order theory has been applied to the problem of flexure of generally orthotropic plates. The performance of the nine-noded Lagrangian isoparametric element has been studied in conjunction

Table 11. Deflections and moments in simply supported plate under uniform loading ($h/a = 0.1$)

	Fibre orientation (degrees)	$w_{max} \frac{E_f^*}{hp}$	$\frac{Max M_x}{h^2 p}$	$\frac{Max M_y}{h^2 p}$
Present higher-order element	30	2121.9	5.843	2.228
	45	1959.1	3.540	3.540
	60	2121.9	2.228	5.843
Mindlin element	30	2081.7	5.674	2.217
	45	1848.5	3.547	3.547
	60	2081.7	2.217	5.674
Elasticity solution [23]	30	2124.0	5.821	2.228
	45	1960.5	3.533	3.533
	60	2124.0	2.228	5.821
Thin plate theory [23]	30	1459.6	5.943	2.268
	45	1302.6	3.603	3.603
	60	1459.6	2.268	5.943

† Young's Modulus for boron fibre (E_f) (psi) = 60×10^6 .
 Max. deflection occurs at centre of plate.
 Max. BMS occur at centre of plate (nearest Gauss point).

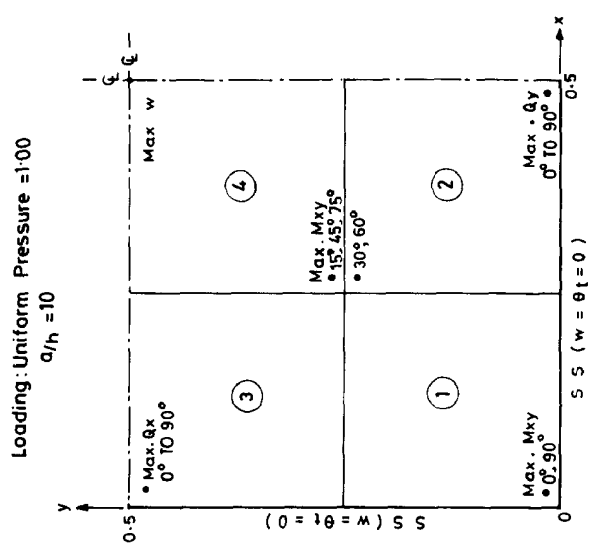


Fig. 8. Locations for critical values of transverse displacement, shear force and twisting moment.

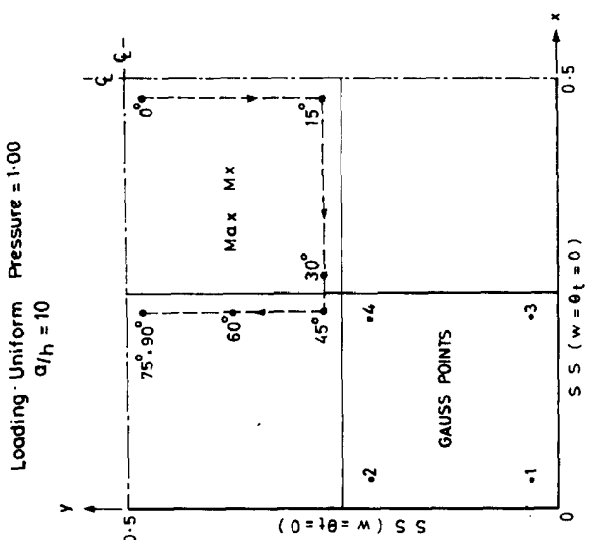


Fig. 9. Locations for critical values of bending moment (M_y).

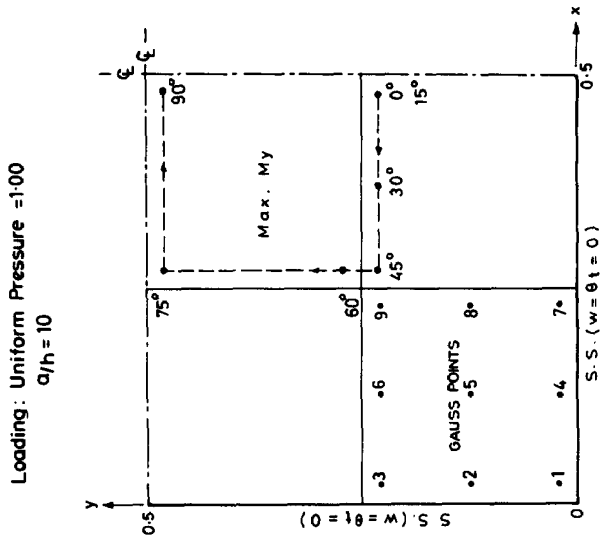


Fig. 10. Locations for critical values of bending moment (M_x).

with the present theory. Examples have been presented giving comparisons with thin plate, elasticity and Mindlin/Reissner solutions. For the examples considered, thin plate theory which neglects transverse shear terms appears to be inadequate. In general, the agreement between results of the elasticity solution and the present higher-order theory was better as compared to Mindlin theory. Qualitatively, this could be due to the better representation of the cross-sectional deformation and the stress-strain law. Errors in the present results can still be reduced by mesh refinement. The results presented for the first time in the form of Figs 2-10 should be of help to all research workers/practising engineers in this field.

REFERENCES

1. S. P. Timoshenko and S. Woinowsky-Krieger, *Theory of Plates and Shells*. McGraw-Hill, New York (1959).
2. R. Szilard, *Theory and Analysis of Plates-Classical and Numerical Methods*. Prentice-Hall, Englewood Cliffs, NJ (1974).
3. O. C. Zienkiewicz, *The Finite Element Method*. McGraw-Hill, Maidenhead, U.K. (1977).
4. R. D. Cook, *Concepts and Applications of Finite Element Analysis*. John Wiley, New York (1981).
5. J. E. Ashton and J. M. Whitney, Theory of laminated plates. In *Progress in Material Science Series, Vol. IV*. Technomic, Stanford, CT (1970).
6. E. Reissner, The effect of transverse shear deformation on the bending of elastic plates. *ASME, J. appl. Mech.* **12**, A69-A77 (1945).
7. R. D. Mindlin, Influence of rotatory inertia and shear deformation on flexural motions of isotropic elastic plates. *ASME, J. appl. Mech.* **18**, 31-38 (1951).
8. S. J. Medwadowski, A refined theory of elastic orthotropic plates. *ASME, J. appl. Mech.* **25**, 437-443 (1958).
9. P. C. Yang, C. H. Norris and Y. Stavsky, Elastic wave propagation in heterogeneous plates. *Int. J. Solids Struct.* **2**, 665-684 (1966).
10. K. H. Lo, R. M. Christensen and E. M. Wu, A high-order theory of plate deformation part I: Homogeneous plates. *ASME, J. appl. Mech.* **44**, 663-668 (1977).
11. K. H. Lo, R. M. Christensen and E. M. Wu, A high-order theory of plate deformation part 2: Laminated plates. *ASME, J. appl. Mech.* **44**, 669-676 (1977).
12. E. Reissner, On transverse bending of plates, including the effects of transverse shear deformation. *Int. J. Solids Struct.* **11**, 569-573 (1975).
13. T. Kant, Numerical analysis of thick plates. *Comput. Meth. appl. Mech. Engng* **31**, 1-18 (1982).
14. T. Kant, D. R. J. Owen and O. C. Zienkiewicz, A refined higher-order C^0 plate bending element. *Comput. Struct.* **15**, 177-183 (1982).
15. N. D. Phan and J. N. Reddy, Analysis of laminated composite plates using a higher-order shear deformation theory. *Int. J. Numer. Meth. Engng* **21**, 2201-2219 (1985).
16. M. Levinson, An accurate, simple theory of the statics and dynamics of elastic plates. *Mech. Res. Commun.* **7**, 343-350 (1980).
17. M. V. V. Murthy, An improved transverse shear deformation theory for laminated anisotropic plates. NASA Technical paper 1903 (1981).
18. J. M. Whitney, Delamination in composite materials. Proceedings of 19th Mid-Western Mechanics Conference, Ohio State University, Columbus, OH, pp. 217-218 (1985).
19. A. K. Gupta and B. Mohraz, A method of computing numerically integrated stiffness matrices. *Int. J. Numer. Meth. Engng* **5**, 83-89 (1972).
20. T. Kant and N. P. Sahani, Fibre reinforced plates-some studies with 9-noded Lagrangion/Heterosis element. Trans. 8th Intl Conf. Struct. Mech. Reactor Technol, paper B 8/7, pp. 315-320 (1985).
21. S. Srinivas and A. K. Rao, Bending, vibration and buckling of simply supported thick orthotropic plates and laminates. *Int. J. Solids Struct.* **6**, 1463-1481 (1970).
22. K. T. S. R. Iyengar and S. K. Pandya, Analysis of orthotropic rectangular thick plates. *Fibre Sci. Technol.* **18**, 19-36 (1983).
23. S. A. Hussainy and S. Srinivas, Flexure of rectangular composite plates. *Fibre Sci. Technol.* **8**, 59-76 (1975).

APPENDIX 1: ELEMENTS OF C MATRIX

$$C_{11} = \frac{E_1(1 - \nu_{32}\nu_{23})}{A}$$

$$C_{12} = \frac{E_2(\nu_{12} + \nu_{13}\nu_{32})}{A} = C_{21}$$

$$C_{13} = \frac{E_3(\nu_{13} + \nu_{12}\nu_{23})}{A} = C_{31}$$

$$C_{22} = \frac{E_2(1 - \nu_{31}\nu_{13})}{A}$$

$$C_{23} = \frac{E_3(\nu_{23} + \nu_{13}\nu_{21})}{A} = C_{32}$$

$$C_{33} = \frac{E_3(1 - \nu_{12}\nu_{21})}{A}$$

$$C_{44} = G_{12}$$

$$C_{55} = G_{23}$$

$$C_{66} = G_{13},$$

where

$$A = (1 - \nu_{23}\nu_{32} - \nu_{12}\nu_{21} - \nu_{13}\nu_{31} - \nu_{12}\nu_{23}\nu_{31} - \nu_{13}\nu_{32}\nu_{21})$$

$$\nu_{21} = \frac{E_2}{E_1}\nu_{12}$$

$$\nu_{32} = \frac{E_3}{E_2}\nu_{23}$$

$$\nu_{31} = \frac{E_3}{E_1}\nu_{13}$$

APPENDIX 2: ELEMENTS OF Q MATRIX

$$Q_{11} = C_{11}c^4 + 2(C_{12} + 2C_{44})c^2s^2 + C_{22}s^4$$

$$Q_{12} = (C_{11} + C_{22} - 4C_{44})c^2s^2 + C_{12}(s^4 + c^4) = Q_{21}$$

$$Q_{13} = C_{13}c^2 + C_{23}s^2 = Q_{31}$$

$$Q_{14} = (C_{11} - C_{12} - 2C_{44})c^3s + (C_{21} - C_{22} + 2C_{44})s^3c = Q_{41}$$

$$Q_{15} = Q_{16} = 0 = Q_{51} = Q_{61}$$

$$Q_{22} = C_{11}s^4 + 2(C_{12} + 2C_{44})s^2c^2 + C_{22}c^4$$

$$Q_{23} = C_{13}s^2 + C_{23}c^2 = Q_{32}$$

$$Q_{24} = (C_{11} - C_{12} - 2C_{44})s^3c \\ + (C_{12} - C_{22} + 2C_{44})sc^3 = Q_{42}$$

$$Q_{25} = Q_{26} = 0 = Q_{52} = Q_{62}$$

$$Q_{33} = C_{33}$$

$$Q_{34} = (C_{31} - C_{32})sc = Q_{43}$$

$$Q_{35} = Q_{36} = 0 = Q_{53} = Q_{63}$$

$$Q_{44} = (C_{11} + C_{22} - 2C_{12} - 2C_{44})s^2c^2 \\ + C_{44}(c^4 + s^4)$$

$$Q_{45} = Q_{46} = 0 = Q_{54} = Q_{64}$$

$$Q_{55} = C_{55}c^2 + C_{66}s^2$$

$$Q_{56} = (C_{55} - C_{66})cs = Q_{65}$$

$$Q_{66} = C_{55}s^2 + C_{66}c^2.$$